Local Octahedral Tilts in $La_{2-x}Ba_xCuO_4$: Evidence for a New Structural Length Scale

S. J. L. Billinge,[1] G. H. Kwei,[1] and H. Takagi[2]
[1]*Los Alamos National Laboratory, Los Alamos, New Mexico 87545*
[2]*Department of Applied Physics, University of Tokyo, Yayoi 2 11 16, Bunkyo-ku, Tokyo 113, Japan*
(Received 11 November 1993)

The short-range structure in $La_{2-x}Ba_xCuO_4$ is examined by obtaining the pair distribution function from neutron powder diffraction data. In contrast to the predictions of the crystal structure models, locally, the CuO_6 octahedra do not change their tilt direction at the low-temperature tetragonal (LTT) to low-temperature orthorhombic (LTO) phase transition: they always tilt in the [110] (LTT) directions. The long-range structures of the high-temperature phases result from coherent superpositions of the local LTT variants. The local tilt order extends over $\sim$ 1 nm. We discuss the implications of this local structure for the properties.

PACS numbers: 74.72.Dn, 61.50.Ks, 61.12.Gz

High-T_c superconductors have extraordinary normal state and superconducting properties; no single theory has emerged which comprehensively explains all of the observations [1]. The structure plays an important role in determining the properties [2] and a detailed understanding of the structure is a prerequisite to a full understanding of these properties. In particular, the structure on nanometer length scales is likely to be important since a number of physical properties have characteristic lengths of this magnitude: for example, antiferromagnetic (AF) spin correlations [3] and superconducting coherence [4]. We have used pair-distribution function analysis (PDF) of neutron powder diffraction data to study the local structure of $La_{2-x}Ba_xCuO_4$. This is one of the few techniques which can yield direct structural information on these nanometer length scales. We find that local atom displacements exist which are subtly different from those predicted by the long-range structure. The local displacements are ordered over lengths of $\sim$ 1 nm. Thus, a structural coherence length exists which is comparable to the correlation lengths associated with the spin and charge systems.

As $La_{2-x}Ba_xCuO_4$ is cooled it undergoes two structural phase transitions. At high temperature the long-range order is described by the high-temperature tetragonal (HTT) structure (space group: $I4/mmm$) [5]. The CuO_2 planes are crystallographically flat. At a temperature T_{d1}, which depends strongly on Ba content, it transforms to the low-temperature orthorhombic (LTO) phase (*Abma*) [6]. Finally, over a restricted range of composition and at temperature T_{d2} ($T_{d2} < T_{d1}$) it transforms into the low-temperature tetragonal (LTT) phase ($P4_2/ncm$) [7]. This is a first order transition; the sample transforms gradually over a $\gtrsim$ 20 °C interval, but remains $\sim$ 5% untransformed even at low temperatures. These transitions have been understood as arising primarily from rigid tilts of the CuO_6 octahedra accompanied by small strains which distort the octahedra. Referred to an *Abma* unit cell, the tilts are about [010] in the LTO phase and [110] directions in the LTT phase. We find that on the local level this picture is not correct: instead the direction and magnitude of tilts depend weakly on temperature, the octahedra *always* tilt about [110], and the long-range order understood from the crystal structure is a *coherent average of the local configurations.*

We have carried out an analysis of $La_{2-x}Ba_xCuO_4$ for $x = 0.125$ and 0.15 using Rietveld [8] and PDF [9] analyses of neutron powder diffraction data. The Rietveld refinements give the long-range structure whereas the PDF analysis yields primarily local structural information. The pair distribution function $G(r)$ is defined as

$$G(r) = \frac{2}{\pi}\int_0^\infty Q[S(Q) - 1]\sin Qr\, dQ, \qquad (1)$$

where $S(Q)$ is the structure function, Q is the momentum transfer of the neutron, and r is a distance in real space. $G(r)$ may be obtained by a Fourier transform of powder diffraction data which have been properly corrected for absorption, multiple scattering, and inelasticity effects and normalized. It provides a direct representation of the instantaneous local structure of a material. Peaks appear in G at positions r corresponding to characteristic atom-atom pair separations (pair correlations) in the crystal. For example, the peak that can be seen in Fig. 1 at $r = 0.19$ nm originates from the Cu to in-plane oxygen (O1) nearest-neighbor correlation. PDFs can be calculated from structural models [10,11] and compared to the data. In the current work we have also used a least-squares minimization technique [10] that allows local structural parameters to be refined against the experimental PDFs.

Sample preparation and characterization have been described elsewhere [12]. Time-of-flight neutron diffraction was carried out on approximately 12.5 g of each sample as a function of temperature using the High Intensity Powder Diffractometer at the Manuel Lujan Jr. Neutron Scattering Center (LANSCE).

The long-range crystal structure models of the *Abma* and $P4_2/ncm$ phases imply that, at the LTO-LTT tran-

0031-9007/94/72(14)/2282(4)$06.00

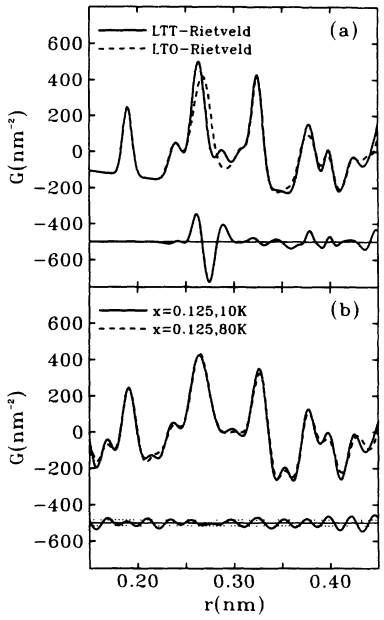

FIG. 1. (a) PDFs calculated from models. The solid line is the LTT crystal structure model; the dashed line is the LTO structure model. A difference plot is shown underneath. (b) PDFs from data collected from the $x = 0.125$ sample in the LTT phase (solid line, 10 K) and in the LTO phase (dashed line, 80 K). A difference is plotted below. The dotted lines indicate the random errors at the 1σ level.

sition, the CuO_6 octahedral tilt axes rotate from [010] to [110]. This change produces large shifts of the apical oxygen [O(2)] ion position which will be clearly visible in the PDF. This is illustrated in Fig. 1(a) which shows *model* PDFs calculated using the LTO and LTT structure models. Lattice parameters and atom coordinates for these models were taken from Rietveld refinements of the long-range structure from the $x = 0.125$ sample when it was in the LTO phase (80 K) and LTT phase (10 K), respectively [12]. In the latter case a two phase refinement was carried out with the sample 95% in the LTT phase and 5% in the LTO phase. The peak at 0.264 nm contains the La-O(2) correlation (marked *A-B* in Fig. 2) which is most sensitive to the local tilt orientation and shows a large change when the local tilts reorient. However, the *experimental* PDFs, shown in Fig. 1(b), show that no change occurs to this peak as the samples go through the LTO-LTT transition. This is further emphasized in Fig. 3(a) which shows the height of the 0.264 nm peak as a function of temperature for both the $x = 0.125$ (squares) and the $x = 0.15$ (circles) sample. The LTO-LTT transition for both these samples is centered about ~ 55 K [12] and indicated by the dashed line in the figure. The peak height varies smoothly through the transition and does not deviate from the expected Debye behavior shown by the solid line. This plot indicates, in a model independent way, that this peak is unaffected by the LTO-LTT transition: there is no reorientation of *local* tilts at this transition. By comparison, the peak at 0.605 nm does

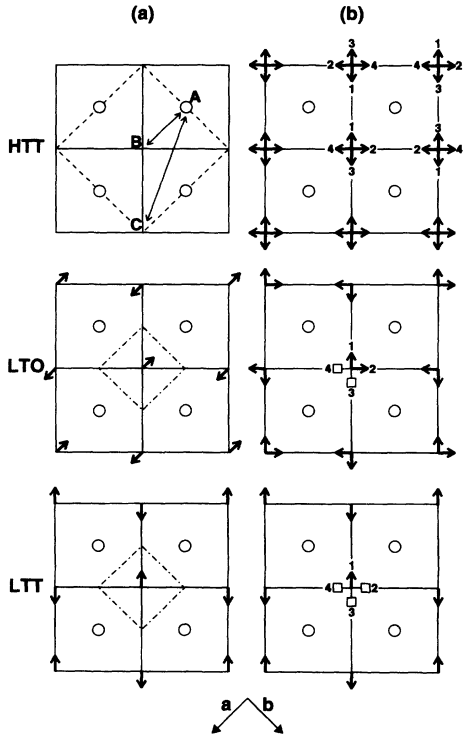

FIG. 2. Schematic illustration of the pattern of octahedral tilts in the various phases. The arrows indicate the tilt directions predicted by (a) the crystal structure models and (b) the local structure models. Cu sits under the apices, La at the positions denoted by open circles. The dashed line outlines the *Abma* unit cell; the dot-dashed lines illustrate the orientation of the CuO_6 octahedra.

sharpen at this transition as shown in Fig. 3(b). This peak contains the La-O(2) *next-nearest-neighbor* correlation. This behavior suggests that the intermediate range ordering of the tilts is changing at this transition rather than the orientation of the tilt axes.

The local tilt direction of the octahedra in the LTO and LTT phases can be determined by refining structure models using the PDF. Both the LTO and LTT models were refined to the $x = 0.125$ data over a range of temperatures from 10 to 300 K. Lattice parameters, atom coordinates, and isotropic thermal factors were refined over the range $0.1 < r < 1.0$ nm with a total of 14 parameters for the LTO and 13 parameters for the LTT refinements. At all temperatures a significantly better fit is obtained from the LTT model than the LTO model. In particular, a much better fit is obtained to the region around 0.26 nm from the LTT model as shown in Fig. 4. This indicates that, locally, the octahedra are always tilted in the LTT sense, even in the *Abma* phase.

The average long-range structure of the *Abma* phase can be understood as a linear superposition of local LTT-like domains. The LTO pattern of displacements is recovered from a linear combination of LTT variants which are rotated by $\pi/2$ with respect to each other around [001]. This is shown schematically in Fig. 2. The pat-

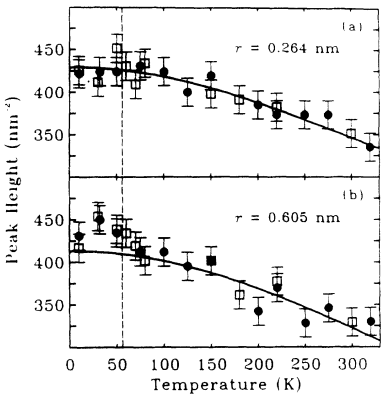

FIG. 3. PDF peak height vs temperature. The open squares and closed circles are from the $x = 0.125$ and $x = 0.15$ samples, respectively. The solid lines are least squares fits of the $x = 0.15$ data to Debye behavior. The vertical dashed line indicates the midpoint temperature T_{d2} where both samples transform to the LTT phase. The Debye fits were carried out for $T > T_{d2}$ and extrapolated. In (a) the height of the peak at 0.264 nm is plotted and in (b) the peak at 0.605 nm.

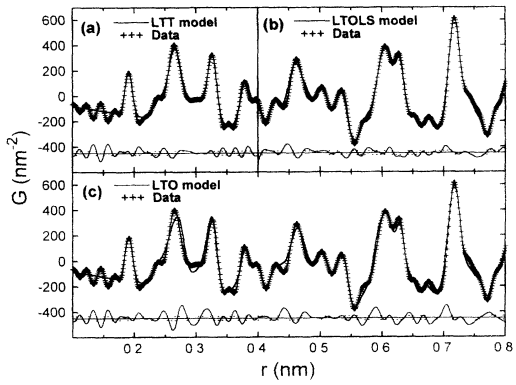

FIG. 4. Refinements of various models to the $x = 0.125$, 80 K data (*Abma* phase). The models are plotted as solid lines and the data as crosses. Difference curves are shown below. The dotted lines indicate the random errors of the data at the 1σ level. (a) LTT, (b) LTOLS, (c) LTO models.

tern of arrows in column (a) (average structure) can be obtained from a vector sum of the arrows in column (b) (local structure), where the arrows indicate the directions of O(2) ion displacements and define the octahedral tilt directions. In analogy with the order-disorder picture used to describe the low-temperature phase transitions in $BaTiO_3$ [13], the low-temperature *Abma* and $P4_2/ncm$ phases occur when the O(2) ions preferentially occupy the [110] displaced sites as indicated in Fig. 2(b). In the high-temperature $I4/mmm$ phase, all four displaced O(2) positions are equally occupied. In the *Abma* phase, sites 1 and 2 of Fig. 2(b) are preferentially occupied and 3 and 4 have a reduced occupancy and in the low-temperature $P4_2/ncm$ phase, site 1 is fully occupied.

This picture was tested against the data by constructing a model with the four-well potential surface described for the O(2) ion. HTTLS and LTOLS (LS = linear superposition) models were defined to describe the $I4/mmm$ and *Abma* phases, respectively, as linear superpositions of local LTT domains as indicated in Fig. 2(b). Details of the modeling will be described later [14]. The HTTLS, LTOLS, and standard LTO and HTT models were refined against the 300, 220, 180, 150, 80, and 10 K data sets over the range 0.4–1.2 nm.

The results of these refinements support the proposed description. Above T_{d1} the HTTLS model gives the best agreement whereas below T_{d1} the LTOLS model does. In addition, the models give a good intuitive description of the continuous HTT-LTO transition. Below T_{d1} the *average* O(2) displacement increases smoothly from zero in the [100] direction. In the new picture, this average tilt angle comes from the center of mass of the local O(2) ion displacements. A nonzero *average* LTO tilt implies a preferential occupancy of the 1 and 2 sites over the 3 and 4 sites. Thus, we expect the refined values of the occupancy of the 1 and 2 sites to increase smoothly on cooling from a value of 0.25 above T_{d1}, saturating at 0.5 at some lower temperature. This is exactly what is observed in the refinements. At 180 K, just below T_{d1} the 1,2 site occupancy parameter refines to $O_1 = O_2 = 0.317$; by 150 K this value has risen to 0.461 and at lower temperatures it remains close to 0.5.

Further, the PDF peak at 0.605 nm, which contains the La-O(2) next-nearest-neighbor correlation (*A-C* in Fig. 2), was fit poorly by both the pure LTT and LTO models at all temperatures below T_{d1} [for example, see Fig. 4(c)] but is well fit by the LTOLS model [Fig. 4(b)]. As we show in Fig. 3(b), this peak sharpens at the LTO-LTT transition. The fact that this peak is sensitive to the LTO-LTT transition, whereas the peak at 0.264 nm is not, is strong evidence that this transition involves a change in the intermediate-range ordering of O(2) displacements (and therefore octahedral tilts) rather than a change in direction of the octahedral tilt axes.

Based on early PDF results [15], Egami *et al.* suggested that tilts about [110] directions should have lower energy than the observed [010] tilts of the LTO structure since O(2) moved closer to two La ions rather than one. This was later confirmed by total energy calculations [16] which predict a four-well potential for the O(2) ion similar to our model. The PDF results show that, locally, the more stable [110] tilts are always present, even in the *Abma* phase and it is the inability of these tilts to order over long range at intermediate and high temperatures which gives rise to the average LTO and HTT structures.

When the LTT tilts are isolated in a single plane they form a quasi-one-dimensional tilt pattern: tilt information propagates easily in the direction of tilting ([110] and $[\bar{1}\bar{1}0]$ in Fig. 2) but not in the perpendicular direction ($[\bar{1}10]$ and $[1\bar{1}0]$). The tilt information is transferred in the perpendicular ($[\bar{1}10]$) direction primarily via small cooperative displacements of the La ions from their

high symmetry positions. However, the average static displacements of these ions are small making this structural link weak. The PDF refinements show that, even at 80 K, the static displacements of La are smaller than its rms thermal displacements; thus, thermal motion can easily frustrate long-range three-dimensional order of the LTT tilts.

The HTT-LTO phase transition in undoped and strontium doped La_2CuO_4 has been explained with a soft-mode picture [7]. An X-point phonon was seen to condense at T_{d1} [17]. This mode was identified as the collective octahedral tilting with the reduced symmetry of the LTO phase. The PDF does not give information directly about the lattice dynamics; it reveals the instantaneous local nuclear density. It shows clearly that at the O(2) site significant nuclear density occurs at the [110] (LTT) displaced positions rather than [010] (LTO) positions. In this case the observed soft modes may result from low frequency collective fluctuations of the tilts between the *displaced* O(2) minima. In the high-temperature phase, hops between all the sites are degenerate. Below T_{d1} the phonon corresponding to 1-4 and 2-3 hops (the numbers are defined in Fig. 2) hardens, making these fluctuations more difficult, whereas the phonon corresponding to 1-2 transitions remains soft [18]. This is consistent with our observation that the 1 and 2 sites [defined in Fig. 2(b)] are both significantly occupied in the LTO phase at the expense of the 3 and 4 sites. It also suggests that the local tilts are fluctuating significantly down to rather low temperatures since the soft modes are low (~ 4 meV) in energy.

Since the local LTT order is probably one dimensional we might expect that the locally ordered domains that form will be long and thin. The $\pi/2$ rotated variants will interleave with each other to produce a tweedlike microstructure similar to that observed in other superconductors and perovskites [19]. Perfect structural coherence only exists within each domain. We can estimate this coherence length from the PDF. Already, in the range $0.4 < r < 1.2$ nm, the linear superposition models give the best agreement. This indicates that significant interdomain correlations exist on this length scale and the shortest dimension of the domains is ~ 1 nm. This is the same magnitude as the coherence length of antiferromagnetic spin fluctuations which have been measured in $La_{2-x}Sr_xCuO_4$ for a similar doping level [3]. Spins couple to the lattice via the spin orbit interaction and they are sensitive to the octahedral tilts [20]. When long-range AF order is suppressed on doping, the local tilt orientations will play an important role in determining the orientation of the dipoles in space. The disruption of the tilt order on intermediate length scales produces an inhomogeneous background which will tend to frustrate the local AF order. In addition we might expect the spins to couple to low energy tilt fluctuations producing local spin reorientations in space.

We have shown that there is a significant random component to the crystal potential in $La_{2-x}Ba_xCuO_4$. Locally, octahedral tilts are about [110] directions and the long-range order in the *Abma* and *I4/mmm* phases comes from a superposition of local tilt variants. This disorder affects carriers directly by increasing the scattering rate and it will have other implications; for example, it will contribute to the Anderson localization of carriers. A new structural length scale of ~ 1 nm has been identified which is similar to the coherence lengths for AF correlations and superconductivity.

We acknowledge helpful discussions with Z. Fisk, J. D. Thompson, and R. Pynn. This work was done under the auspices of the U.S. Department of Energy through Contract No. W-7405-ENG-36 with the University of California.

[1] See, for example, *Physical Properties of High-Temperature Superconductors*, edited by D. M. Ginsberg (World Scientific, Singapore, 1988–1992), Vols. I–III.
[2] See, for example, *Proceedings of the Conference on Lattice Effects in High-T_c Superconductors*, edited by Y. Bar-Yam *et al.* (World Scientific, Singapore, 1992).
[3] R. J. Birgeneau *et al.*, Phys. Rev. B **39**, 2868 (1989).
[4] M. Suzuki and M. Hikita, Jpn. J. Appl. Phys. **28**, L1368 (1989); B. Batlogg, in *High Temperature Superconductivity*, edited by K. S. Bedell *et al.* (Addison-Wesley, Redwood City, 1990), p. 66.
[5] J. D. Jorgensen *et al.*, Phys. Rev. Lett. **58**, 1024 (1987).
[6] D. McK. Paul *et al.*, Phys. Rev. Lett. **58**, 1976 (1987).
[7] J. D. Axe *et al.*, Phys. Rev. Lett. **62**, 2751 (1989).
[8] A. C. Larson and R. B. Von Dreele, Los Alamos National Laboratory Report No. LA-UR-86-748, 1987 (unpublished).
[9] T. Egami, Mater. Trans. **31**, 163 (1990).
[10] S. J. L. Billinge and T. Egami, Phys. Rev. B **47**, 14386 (1993).
[11] B. H. Toby and T. Egami, Acta. Crystallogr. Sect. A **48**, 336 (1992).
[12] S. J. L. Billinge *et al.*, Phys. Rev. Lett. **71**, 1903 (1993).
[13] R. Comes *et al.*, Solid State Commun. **6**, 715 (1968).
[14] S. J. L. Billinge, G. H. Kwei, and H. Takagi (unpublished).
[15] T. Egami *et al.*, Rev. Solid State Sci. **1**, 247 (1987).
[16] W. E. Pickett, R. E. Cohen, and H. Krakauer, Phys. Rev. Lett. **67**, 228 (1991); and in *Proceedings of the Conference on Lattice Effects in High-T_c Superconductors* (Ref. [2]), p. 217.
[17] R. J. Birgeneau *et al.*, Phys. Rev. Lett. **59**, 1329 (1987).
[18] T. R. Thurston *et al.*, Phys. Rev. B **39**, 4327 (1989).
[19] J. A. Krumhansl, in *Proceedings of the Conference on Lattice Effects in High-T_c Superconductors* (Ref. [2]), p. 503.
[20] N. E. Bonesteel, T. M. Rice, and F. C. Zhang, Phys. Rev. Lett. **68**, 2684 (1992).